2010

Apoptosis Initiation and Angiogenesis Inhibition: Melanoma Targets for Nanosecond Pulsed Electric Fields

Xinhua Chen
Old Dominion University

Juergen F. Kolb
Old Dominion University, jkolb@odu.edu

R. James Swanson
Old Dominion University

Karl H. Schoenbach
Old Dominion University, kschoenb@odu.edu

Stephen J. Beebe
Old Dominion University, sbeebe@odu.edu

Original Publication Citation

Chen, X. H., Kolb, J. F., Swanson, R. J., Schoenbach, K. H., & Beebe, S. J. (2010). Apoptosis initiation and angiogenesis inhibition: Melanoma targets for nanosecond pulsed electric fields. *Pigment Cell & Melanoma Research, 23*(4), 554-563. doi:10.1111/j.1755-148X.2010.00704.x

Apoptosis initiation and angiogenesis inhibition: melanoma targets for nanosecond pulsed electric fields

Xinhua Chen[1], Juergen F. Kolb[1], R. James Swanson[1,2], Karl H. Schoenbach[1] and Stephen J. Beebe[1,3]

1 Frank Reidy Research Center for Bioelectrics, Old Dominion University, Norfolk, VA, USA **2** Department of Biology, Old Dominion University, Norfolk, VA, USA **3** Department of Physiological Sciences, Eastern Virginia Medical School, Norfolk, VA, USA

CORRESPONDENCE Stephen J. Beebe, e-mail: sbeebe@odu.edu

KEYWORDS electric fields/non-thermal effects/apoptosis/angiogenesis/caspases/DNA damage/DNA double strand breaks

PUBLICATION DATA Received 3 February 2010, revised and accepted for publication 30 March 2010, published online 2 April 2010

doi: 10.1111/j.1755-148X.2010.00704.x

Summary

Many effective anti-cancer strategies target apoptosis and angiogenesis mechanisms. Applications of non-ionizing, nanosecond pulsed electric fields (nsPEFs) induce apoptosis in vitro and eliminate cancer in vivo; however in vivo mechanisms require closer analysis. These studies investigate nsPEF-induced apoptosis and anti-angiogenesis examined by fluorescent microscopy, immunoblots, and morphology. Six hours after treatment with one hundred 300 ns pulses at 40 kV/cm, cells transiently expressed active caspases indicating that caspase-mediated mechanisms. Three hours after treatment transient peaks in Histone 2AX phosphorylation coincided with terminal deoxynucleotidyl transferase dUTP nick end labeling positive cells and pyknotic nuclei, suggesting caspase-independent mechanisms on nuclei/DNA. Large DNA fragments, but not 180 bp fragmentation ladders, were observed, suggesting incomplete apoptosis. Nevertheless, tumor weight and volume decreased and tumors disappeared. One week after treatment, vessel numbers, vascular endothelial growth factor (VEGF), platelet derived endothelial cell growth factor (PD-ECGF), CD31, CD35 and CD105 were decreased, indicating anti-angiogenesis. The nsPEFs activate multiple melanoma therapeutic targets, which is consistent with successes of nsPEF applications for tumor treatment in vivo as a new cancer therapeutic modality.

Introduction

Many chemotherapeutic and ionizing radiation treatments demonstrate anticancer efficacy, but efforts must continue to find new approaches to address cancer diseases. Six major hallmarks of cancer have been outlined as physiological anomalies that are common to all cancers (Hanahan and Weinberg, 2000) and serve as therapeutic targets. These include evading apoptosis, self sufficiency in growth signals, insensitivity to anti-growth

Significance

Skin cancer is widespread and metastatic melanoma, which is resistant to a wide range of treatment modalities, is the most deadly. Nanosecond pulsed electric fields (nsPEFs) eliminate melanoma by applying extremely brief and intense electric fields, which are high in power but low in thermal energy. The nsPEFs interact with multiple intracellular and plasma membrane structures/functions including apoptosis and anti-angiogenesis mechanisms, both major cancer treatment targets. Applications of nsPEFs are expected to be safe and non-toxic. They can probably be applied using local anesthetic alone or in combination with other treatment modalities and with development of catheter electrodes they can probably be used to treat internal organs with laparoscopic surgery.

signals, sustained angiogenesis, limitless replicative potential, and tissue invasion and metastasis. Kroemer and Pouyssegur (2008) added evading immune surveillance as a seventh cancer hallmark. While many of these hallmarks have been addressed with therapeutic strategies, a number of therapies have focused on activating apoptosis and inhibiting angiogenesis. These include using monoclonal antibodies, recombinant ligands, RNA interference and small molecule antagonists/agonists. However, some of these may promote cellular compensation that leads to resistances and reoccurrences (Fesik, 2005; Letai, 2008). Although cancer death rates have begun to slowly decrease, metastatic melanoma is one of the most resistant cancers. It is appropriate to find alternative treatments and to look beyond pharmaceutical methodologies.

Some alternative therapeutic approaches in clinical trials use physical methods because they locally treat tumors without systemic disturbances. Two such methods, cryotherapy and radiofrequency ablation, use extreme temperatures to induce frank necrosis including (Bland et al., 2007). Several new strategies use electric fields to eliminate cancer. One approach in clinical trials is electro-gene therapy, which uses conventional electroporation (EP) to deliver genes that locally activate immune mechanisms against melanoma (Daud et al., 2008). Another EP technology in clinical application is electrochemotherapy, which delivers impermeable chemotherapeutic drugs to tumors (Gehl, 2008; Heller et al., 1996; Mir et al., 1991). Another physical approach is irreversible EP, which extends EP conditions to fatally damage tissues (Davalos et al., 2005; Lee and Kolodney, 1987; Lee et al., 2000; Maor et al., 2009; Onik et al., 2007).

Another emerging alternative non-drug, non-thermal method extends EP using ultrashort, intense pulsed electric fields with nanosecond durations (nsPEFs) as a non-ionizing means to treat cancer (Beebe et al., 2002, 2003a, 2004; Nuccitelli et al., 2006, 2009). This pulse power technology, initially developed for aerospace and military purposes, has recently crossed disciplines finding potential applications in biology and medicine. Both modeling evidence in vitro (Gowrishankar and Weaver, 2006; Gowrishankar et al., 2006; Hu et al., 2005; Stewart et al., 2004; Vernier et al., 2006) and in vivo (Esser et al., 2009; Gowrishankar et al., 2006; Joshi et al., 2007) and experimental evidence (Schoenbach et al., 2001; Tekle et al., 2005; White et al., 2004) indicate that the larger nsPEFs induce intracellular membrane charging events, which are absent during EP. Further, these same studies indicate that nsPEFs produce nanopores ($\sim$1 nm) in all cell membranes, including plasma membranes (Pakhomov et al., 2009). These differences from EP provide new possibilities for unique cellular effects and some of these may have clinical relevance in cancer (Beebe et al., 2002, 2003a,b, 2004; Chen et al., 2009; Garon et al., 2007; Nuccitelli et al., 2006, 2009) wound healing (Zhang et al., 2008) and cardiovascular medicine (Wang et al., 2009). Thus, EP technology has branched into a number of potentially important clinical cancer applications for gene delivery, drug delivery (electrochemotherapy), irreversible EP and nsPEFs.

The pervasive effects induced by nsPEFs on cell structures and subsequent functions provide potentials for therapeutic applications. One investigated response to nsPEFs (Beebe et al., 2003a,b, 2004; Ford et al., 2010; Hall et al., 2007a) is the appearances of characteristics of apoptosis (Kroemer et al., 2009). In vivo studies have shown nsPEFs to reduce fibrosarcoma tumor size (Beebe et al., 2002, 2003a, 2004), to eliminate B16f10 melanoma in mice without reoccurrence (Nuccitelli et al., 2006, 2009) and to eradicate a human basal cell carcinoma (Garon et al., 2007). We investigated in detail nsPEFs on in vivo mechanisms that permanently remove B16f10 melanoma tumors without reoccurrence in a mouse model (Nuccitelli et al., 2009). The results indicate that nsPEFs target two of the seven cancer hallmarks (Hanahan and Weinberg, 2000; Kroemer and Pouyssegur, 2008) on solid B16f10 melanoma tumors, including apoptosis evasion and sustained angiogenesis, which is critical for a third hallmark, invasion and metastasis.

Results

Tumors were treated in vivo with 100 pulses at 300 ns and 40 kV/cm and analyzed for the presence of Histone 2AX phosphorylation (γH2AX), terminal deoxynucleotidyl transferase dUTP nick end labeling (TUNEL) and active executioner caspase-positive tumor cells in the first hours (1, 3, 6 and 24 h) after treatment. Representative experiments are illustrated in Figure 1 and statistical analyses in Figure 2.

nsPEFs induce DNA double stranded breaks

The presence of γH2AX immunofluorescent staining was used as a sensitive and early monitor to identify DNA at double strand breaks (Bonner et al., 2008; Rogakou et al., 1999) in nsPEF-treated B16f10 tumors in vivo (Figures 1 and 2). Figure 1 shows time-dependent increase in γH2AX in melanoma, with significant differences occurring at 1 h, reaching a peak at 3 h and decreasing to control levels thereafter. A quantitative analysis of γH2AX illustrated in Figure 2 shows that 15, 85, 5 and 5% of B16f10 tumors cells exhibited γH2AX at 1, 3, 6 and 24 h, respectively, after nsPEF treatment.

nsPEFs induce DNA damage determined by TUNEL and agarose gel electrophoresis

Terminal deoxynucleotidyl transferase dUTP nick end labeling is used to define DNA damage and fragmentation as an apoptosis marker (Kroemer et al., 2009). In Figure 1, nsPEF treatment of B16f10 tumors in vivo resulted in significant increases TUNEL positive cells at 3 h post-pulse with a peak near 6 h and decreases by 24 h. Figure 2 indicates that 7, 27, 43 and 3% of

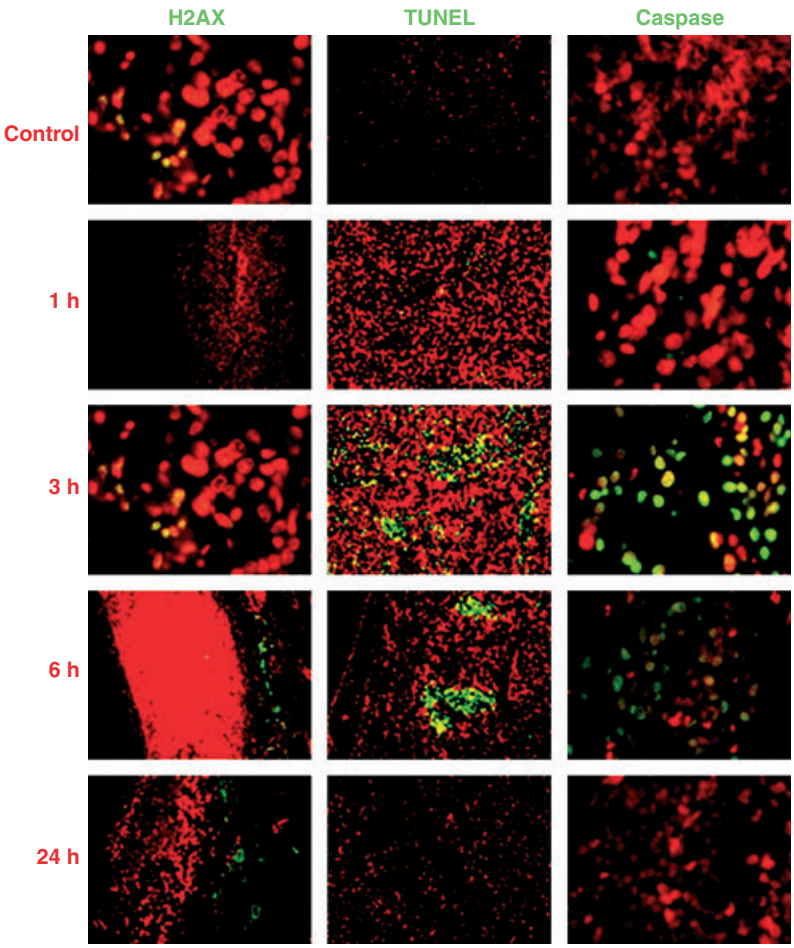

Figure 1. Immunofluorescent staining of γH2AX, terminal deoxynucleotidyl transferase dUTP nick end labeling (TUNEL) and executioner (-3, -6, and -7) caspase positive B16f10 melanoma tumor cells after treatment with nanosecond pulsed electric fields. B16f10 tumors were treated with one hundred 300 ns pulses at 40 kV/cm. One, 3, 6 and 24 h later tumors were removed and prepared for immunofluorescent histology. Representative fluorescent images from each fluorescent antibody condition are shown. Six different mice were used at each time point and each experiment was repeated twice (12 tumors). The γH2AX-, TUNEL- and caspase-positive signals are indicated by green fluorescence in contrast to propidium iodide red fluorescence-stained nuclei. Merged images are indicated as yellow-orange. Magnification is 200×.

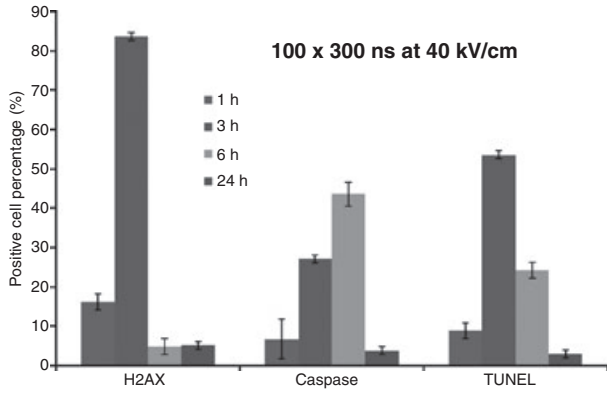

Figure 2. A composite graphic kinetics of DNA damage and apoptosis in the first 24 h after treatment with nanosecond pulsed electric fields. Tumors were treated in vivo, removed at various times and analyzed for immunofluorescent changes in γH2AX, terminal deoxynucleotidyl transferase dUTP nick end labeling (TUNEL) and executioner caspase-3, -6, and -7. Six different mice were used at each time point and each experiment was repeated twice (12 tumors). The results represent the mean ± SD. Significant increases for H2AX at 1 and 3 h and for TUNEL and caspase at 3 and 6 h were $P < 0.001$ versus control.

B16f10 tumor cells were TUNEL positive 1, 3, 6 and 24 h, respectively, after nsPEFs treatment.

To determine whether DNA fragmentation occurred after nsPEF treatment, DNA was extracted from tumors and analyzed by electrophoresis on ethidium bromide-stained agarose gels for multiples of ~180 bp fragments. Typical DNA fragmentation ladders were not present at any times tested. Degraded DNA was observed as large fragments at 6 h and significant DNA smearing at 24 h post-pulse (data not shown).

nsPEFs activate executioner caspases

Immunofluorescent staining for executioner (also called effector) caspase, which cleave cellular proteins to initiate the apoptosis process, was determined using a mixture of antibodies to active caspase-3, -6, and -7 in melanomas at times after nsPEF treatment (Figures 1 and 2). Time courses indicated that percentages of caspase positive cells significantly increased 3 h post-pulse, peaked near 6 h, and then decreased by 24 h. A quantitative analysis of active caspases shown in Figure 2 indicated that 5, 28, 43 and 3% were present 1, 3, 6 and 24 h, respectively, after nsPEF treatment.

Effects of nsPEFs on nuclear morphology

To determine morphological effects on B16f10 nuclei, the nuclear areas were measured after H&E staining at various times after nsPEF treatment (Figure 3). Control tumor cells exhibited light staining pleomorphic nuclei and abundant cytoplasm containing finely dispersed melanin granules. Treated tumors exhibited dense staining, condensed and elongated nuclei. In contrast, treated melanomas exhibited individual cells scattered from tumor cords with coarse intracellular melanin granules and aggregated extracellular melanin granules. Quantitative comparisons were made by calculating mean nuclear area (μm^2) between control melanomas and treated tumors during the first 24 h post-nsPEF treatment. Significant differences were observed between control and all post-treatment times (Figure 3).

Tumor weight decreases after nsPEF treatment

Prior to treatment with nsPEFs melanomas grew to similar weights 6 d after B16f10 tumor initiation (control group 1.45 ± 0.15 versus treated group 1.59 ± 0.12). One day after nsPEF treatment, treated tumors (1.41 ± 0.18) became slightly smaller than control tumors (1.61 ± 0.25), which increased slightly. One week later, tumors without nsPEF treatment increased twofold in weight (2.71 ± 0.17) while treated tumors decreased in weight (0.58 ± 0.21) about threefold.

nsPEFs decrease pre-existing blood supply

As melanoma tumors developed to 5–7 mm^2, a rich blood supply to the tumors with branching vessels was seen by transillumination. In untreated tumors primary and secondary vessels feeding the tumor increased 43, 71, 85 and 100% on days 1, 2, 7, 14, and 17, respectively. In treated tumors, the number of feeding vessel did not decrease until between days 3 and 7. At day 7, vessel numbers were 16% of the same day control. On days 14 and 17, the numbers of vessels feeding the tumor were less than 1% of controls (data not shown).

The vessel numbers within tumors were counted following H&E staining (Figure 4). In untreated tumors, angiogenesis produced expanding endothelial plexuses in red (Figure 4A, B). A decrease in vessel numbers within tumors did not decrease until between days 3 and 7. The decrease in vessel numbers feeding tumors was 33, 50, and 68% on days 7, 14, and 17. In the treated tumors on day 1 and day 2 post-nsPEF treatments, the vasculature still consisted of a fine, reticulated network of small diameter vessels which stained red. On days 7 and 14 vessel numbers decreased dramatically

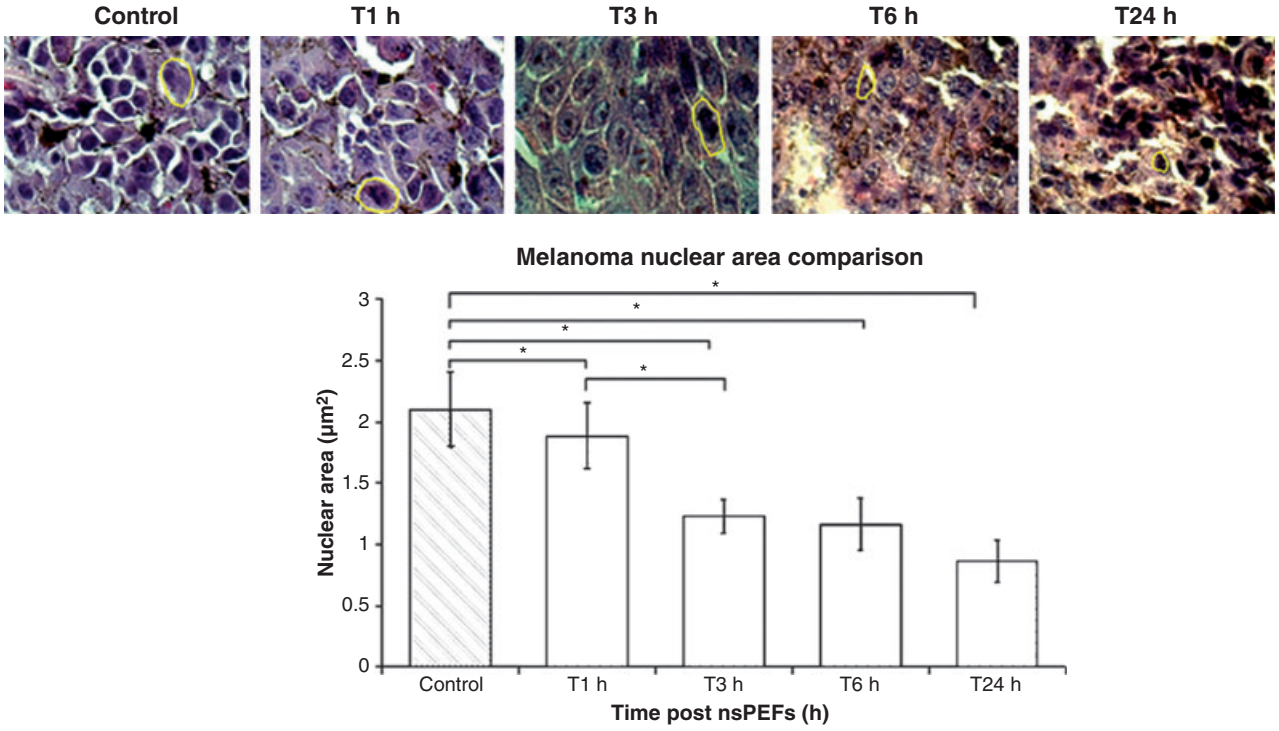

Figure 3. Tumor construction and nuclear shape changes 1–24 h post-nanosecond pulsed electric field treatment. Tumors were treated in vivo with 100 pulses at 300 ns and 40 kV/cm. Tumors were removed 1, 3, 6, and 24 h post-pulses and prepared for H&E staining. Representative samples are shown with 1000× magnification and typical nuclei are outline in yellow. Specimens were randomly analyzed and mean nuclei areas were measured from six mice for each time point and shown in the bar graph with mean and SE using a computer-assisted interactive image analysis system MATLAB. Nuclear areas were estimated after manual editing of binary images. There were significant differences between the control and 1, 3, 6, and 24 h post-pulses ($P < 0.001$) as well as between 1 and 3 h ($P < 0.001$).

with decreased tumor size. On day 17 after nsPEF treatment, tumors shrank to a mass of melanin without red stained vessel lumens. In untreated tumors, growth was accompanied by increased vascularity; the vessel numbers on days 1, 2, 7, 14, and 17 d after nsPEF treatment were significantly increased.

Vascular endothelial growth factor (VEGF) and platelet derived endothelial cell growth factor (PD-ECGF) protein expression were decreased by nsPEF treatment

Neo-vascular markers were assayed including expression of VEGF and PD-ECGF by immunoblot analysis from four tumors from different mice. Both VEGF and PD-ECGF protein expression decreased after nsPEF treatments compared to controls (Figure 5).

nsPEFs inhibit micro-vessel density (MVD)

Common angiogenesis MVD were evaluated by expression of CD31, CD34, and CD105. CD31 is a platelet-endothelial cell adhesion molecule used as a pan-endothelial cell marker. CD34 is an endothelial cell marker. CD105 is a proliferation-related endothelial cell marker. Figure 6 shows typical immunohistochemical expression patterns for each MVD marker. In all three stains, control tumors showed red stained areas indicating the presence of intensive endothelium in neovascular hot spots. Upon high power analysis, red stained areas were seen as endothelial cells or clusters clearly separate from adjacent non-stained tumor cells. In contrast, treated tumors showed significantly attenuated levels of endothelium. A quantitative analysis of MVD markers 1 week after nsPEF treatment indicated greatly significantly reduced staining for all three MVD markers (Figure 6).

Discussion

These studies present a thorough and coordinated analysis that broadens understandings of in vivo

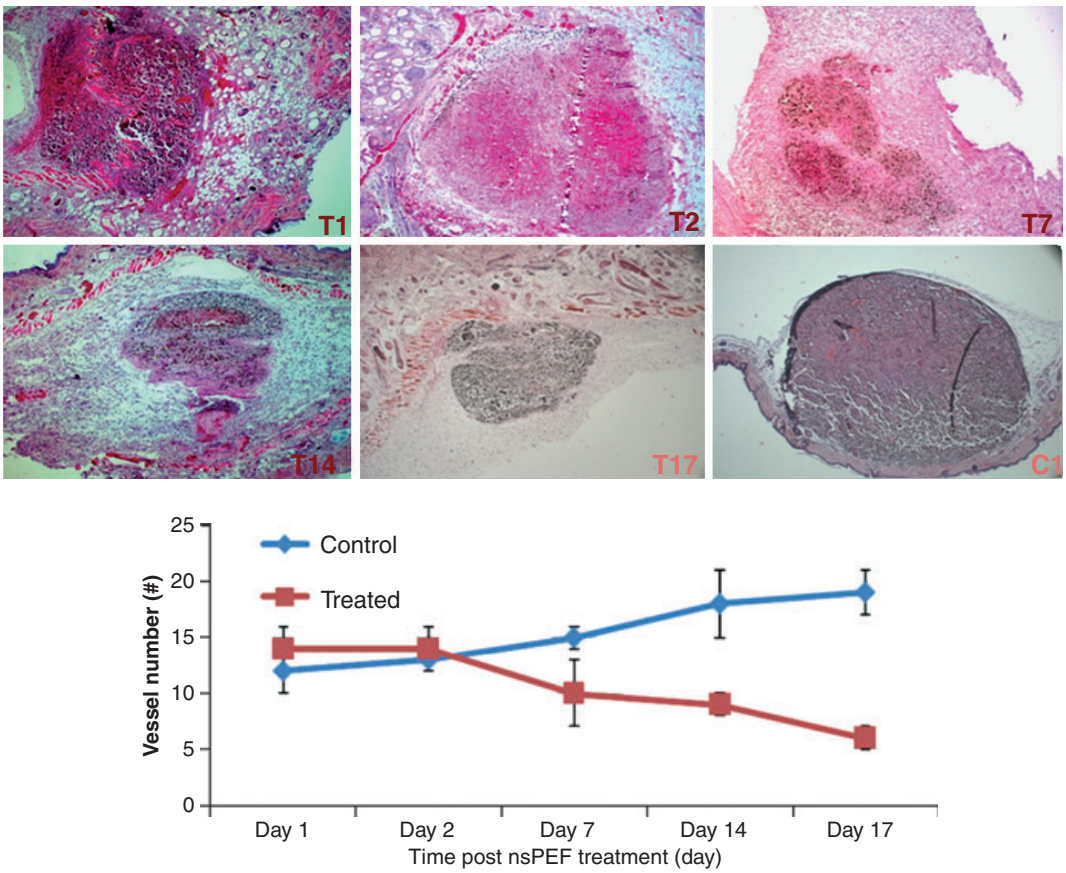

Figure 4. Quantitative analysis of vasculature changes within B16f10 melanoma tumors after the nanosecond pulsed electric field (nsPEF) treatment. Treated tumors were removed on days 1, 2, 7, 14 and 17 after treatment with nsPEFs, shown as T1, T2, T7, T14, and T17; C1 represents control (untreated) tumor. Tumor slides were stained with H&E and tumor vessels were counted by the number of vessel lumen exhibiting red endothelial plexuses (Image Tool; University of Texas, San Antonio, TX, USA). Vessels were counted on areas of 0.74 mm^2 per field on 10 different slides from each sample.

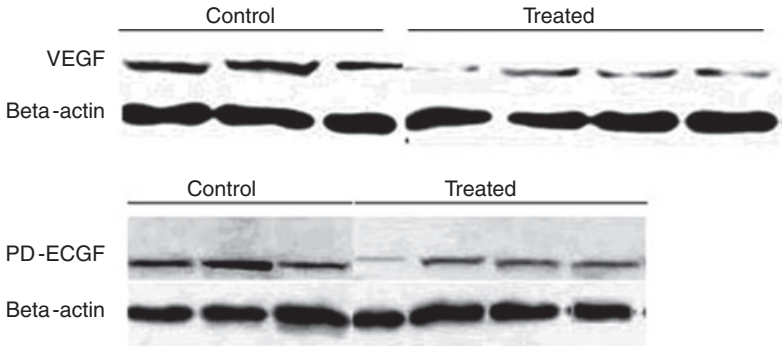

Figure 5. Effect of nanosecond pulsed electric fields (nsPEFs) on vascular endothelial growth factor (VEGF) and PD-ECGF expression after treatment with nsPEFs. VEGF and PD-ECGF protein expression were analyzed by Immunoblot. Three mice bearing control tumors and treated tumors were euthanized 7 d after treatment with nsPEFs. Three control tumors and four treated tumors were analyzed. Beta-actin served as a loading control.

mechanisms for nsPEF-induced cell death in murine B16f10 melanoma (Chen et al., 2009; Nuccitelli et al., 2006, 2009). Both apoptosis and angiogenesis are targets for treatment of cancer cells that establish a niche, perpetuate mass, and construct tumors using host blood supplies. Unlike chemotherapeutic agents, which have systemic effects, nsPEFs are applied as a local treatment, with cells affected depending on the electrode design and pulsing conditions in a treatment zone. There are different sensitivities to nsPEFs for cell types (Beebe et al., 2004; Hair et al., 2003; Stacey et al., 2003) and cell cycle phase (Hall et al., 2007b), and some

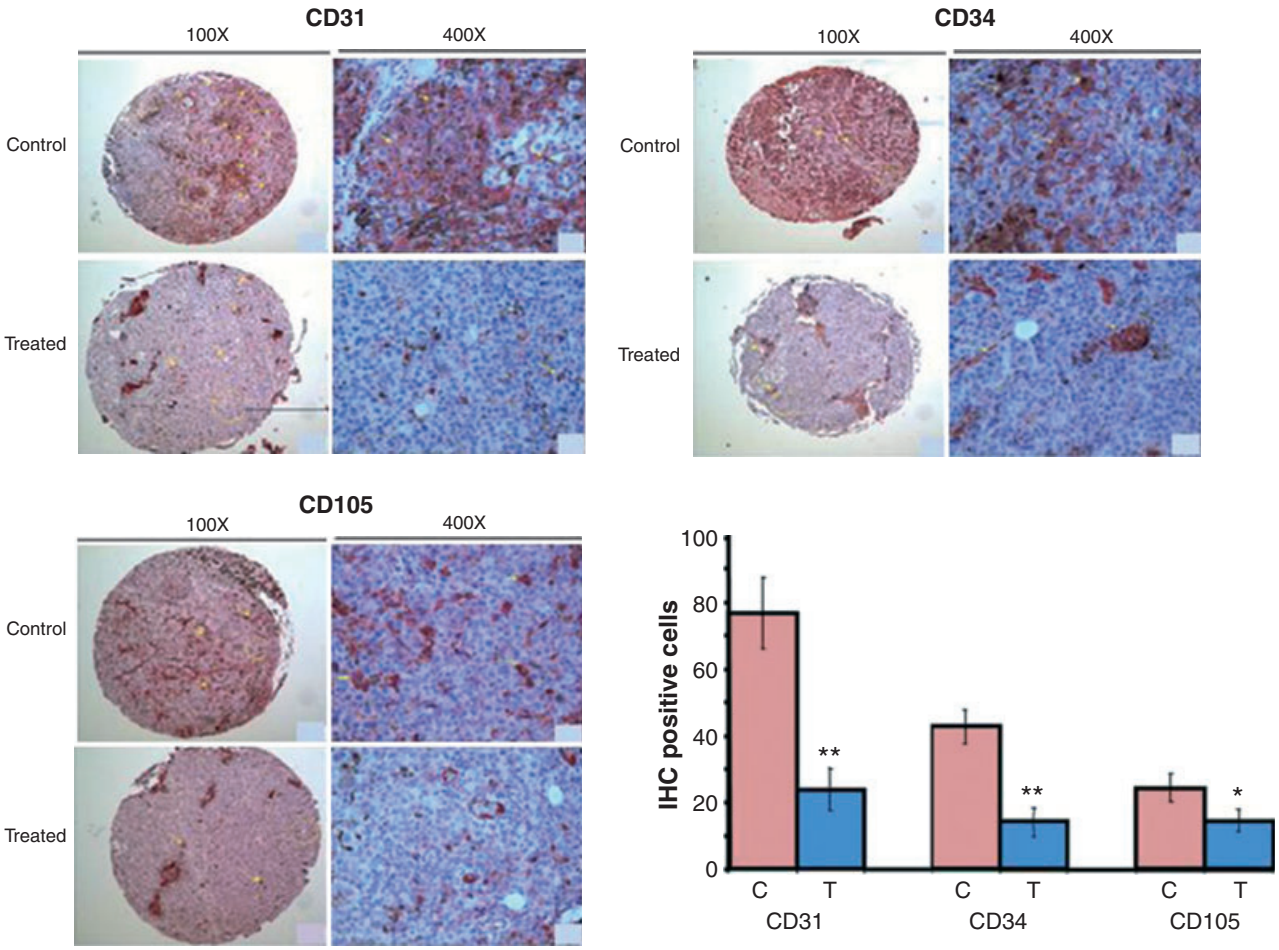

Figure 6. Effect of nanosecond pulsed electric fields (nsPEFs) on micro-vascular density (MVD) by CD31, CD34 and CD105: Top panels and the lower left panel show representative immunohistological staining of MVD markers 7 d after treatment with nsPEFs. The lower right shows quantitative analyses of MVD markers 7 d post-treatment by counting in five different random fields showing the mean and SD. CD-31 (**$P < 0.0001$); CD34 (**$P < 0.0001$) and CD105 (*$P < 0.05$).

of these may have clinical significance. When pulsing conditions reach a cell death threshold, all cells within a treatment zone can be eliminated, including cancer cells, cancer stem cells and corrupted host cells collaborating with tumor cells. This may afford advantages to nsPEFs, since chemotherapeutic agents and ionizing radiation selectively affect proliferating cancer cells and normal proliferating cells, which cause toxic side effects. Mechanisms for nsPEF-induced tumor cell death include caspase-associated apoptosis and caspase-independent apoptosis as well as anti-angiogenic effects as tumors shrink.

Induction of caspase-associated apoptosis appears to be an early nsPEF-induced mechanism that promotes tumor demise as indicated by activation of executioner caspases, which remain active for more than 6 h after treatment. However, apoptosis does not go to completion as indicated by the presence of large DNA fragments and absence of ~180 bp DNA fragments on agarose gels, a late stage apoptosis marker (Kroemer et al., 2009). Treated tumor weight decreases by only 10% during the first day. However, with large numbers of caspase substrates (Fischer et al., 2003) and rapidity of apoptosis (Green, 2005), it is anticipated that substantial disassembly takes place, providing a potential advantage for eventual tumor removal. An in vivo tumor mass is too substantial to be removed quickly by natural endogenous apoptosis mechanisms. Nevertheless, tumor masses decreased after treatment until the tumors were essentially absent within 2–3 weeks.

The inability to remove apoptosing cells leads to secondary necrosis with at least two outcomes (Silva et al., 2008). Leakage of cytosolic contents can lead to inflammation and tissue damage, which is avoided by removal of apoptosing cells. However, in the case of cancer, this takes place within the tumor mass. Likewise, secondary necrotic cells can be taken up by antigen presenting cells, which provides a possibility for immunity. While both outcomes may be advantageous, immunity is rarely realized as a consequence of cancer treatment, but not unprecedented (Daud et al., 2008).

While nsPEFs induce DNA damage (Beebe et al., 2002, 2003a, 2004; Nuccitelli et al., 2006, 2009), cause and effect relationships between active caspases and DNA damage have not been established. Morphologic and molecular evidence suggests that initial DNA damage is caspase-independent. Pyknosis, chromosomal condensation, γH2AX and TUNEL positive cells were present before caspase activation reached its peak. Although γH2AX serves as assembly foci for recruitment of DNA repair mechanisms (Shiloh, 2003), DNA double stranded breaks were identified but not repaired. Early DNA damage does not appear to be a caspase-associated apoptosis marker. However, the mechanism(s) remain to be defined. The nsPEFs do not generate sufficient energy to break hydrogen bonds and nsPEFs are not expected to generate reactive oxygen species (ROS) through ionization of water. Moreover, ROS in B16f10 cells exposed to nsPEFs in vitro were absent (Ford et al., 2010). Since ATM (ataxia telangiectasia mutated) and ATR (ATM and Rad 3-related) kinases are activated with ionizing radiation and UV light (Christmann et al., 2003), knowing the kinase(s) responsible for γH2AX would shed new light on the mechanism(s) for nsPEF-induced DNA damage.

Available data suggest that nsPEF-induced DNA damage is not likely a major cause of caspase-associated apoptosis. First the presence or absence of p53, which regulates transcription-dependent and independent events in response to DNA damage (Sheikh et al., 1998), did not influence survival in HCT116 colon carcinoma cells after nsPEF treatment (Hall et al., 2007a). Second, it is likely that transcription events may be irrelevant in response to nsPEFs, because nsPEF-induced cell death ensues very rapidly (Ford et al., 2010; Nuccitelli et al., 2006) and apoptosis can initiate without transcription. Finally, p53 responses are mediated by mitochondria release of pro-apoptotic factors, which were not evident in nsPEF-treated cells in vitro (Ford et al., 2010). This remains to be determined in vivo. One DNA damage mechanisms could be due to activation of LEI (leukocyte elastase inhibitor)/LEI-derived DNase II resulting in caspase-independent apoptosis with activation of other proteases (Torriglia and Lepretre, 2009). This mechanism is consistent with caspase-independent DNA damage and absences of 180 bp DNA fragments.

Other effects of nsPEFs on DNA and nuclei have been reported as disruption of intra-chromatin granule clusters, suggesting modulation of pre-mRNA splicing mechanisms (Chen et al., 2007). Another possibility is that nsPEFs could disrupt the integrity of dynamic capping structures at chromosome ends, unmasking them, which could appear as damaged DNA (Deng and Chang, 2007). These could be caused by nsPEF-induced conformational changes. Further studies are necessary to determine nsPEF-induced DNA damage mechanism(s).

A second nsPEF therapeutic target is angiogenesis. First, there is significant effects on tumor blood vessels within the treatment zone (Nuccitelli et al., 2006; this study) causing a near immediate tumor infarction. Second, a decrease in vessel numbers supplying tumors is coincident with decreased tumor masses, suggesting tumor-driven angiogenesis. Third, 1 week after treatment there are diminished levels of VEGF, the most ubiquitous pro-angiogenic factor. Vascular endothelial growth factor is a requirement for the angiogenic switch, is a limiting factor for multistage carcinogenesis (Hanahan and Weinberg, 2000) and is induced under ischemic conditions (Bergers and Benjamin, 2003). This is clearly a harbinger for the absence of revascularization and renewed tumorigenesis. This is borne out by elimination of melanoma

and absences of reoccurrences (Nuccitelli et al., 2009). Reduced levels of PD-ECGF, a well known chemotactic factor for vascular endothelial cells, provide further evidence that nsPEFs deplete the melanoma environment of needed angiogenic factors. Moreover, there are significant downstream VEGF effects with reductions in MVD markers CD31, CD34, and CD105. This is consistent with findings that while melanoma tumors shrink and vessel numbers are significantly reduced, formation of new vessels is significantly inhibited. These data indicate that nsPEFs have profound effects to discourage tumor formation and revascularization.

The nsPEF treatment affected both immediate and delayed blood vessel effects, most likely by different mechanisms. One of these could be due to direct electric field-mediated formation of nanopores in fragile endothelial cell membranes in capillaries and small blood vessels. Delayed effects could be due to death of tumor cell-supported angiogenesis, caspase-associated apoptosis and/or deleterious effects on vasa vasorum, small blood vessels that supply large vessels.

The nsPEFs provide a unique electrical-biological interface using high power and low energy to affect plasma membranes and intracellular membranes (this study, Beebe et al., 2002, 2003a,b, 2004). It provides a highly localized treatment that specifically targets entire melanoma tumors within an effective electric field to induce apoptosis, tumor infarction and prevent angiogenesis. Other advantages of nsPEFs include insignificant thermal effects (Nuccitelli et al., 2006), which differentiate it from cryotherapy and radiofrequency ablation. Further, while surgical resections are common for superficial melanoma, applications of nsPEFs did not leave scars on mice (Nuccitelli et al., 2006) or on human skin (unpublished clinical study). The nsPEFs completely eliminated mouse B16f10 melanoma in vivo (Nuccitelli et al., 2006, 2009; this study) and effectively induced apoptosis and induced apoptosis in a number of cancer cell lines in vitro (Beebe et al., 2002, 2003a,b, 2004; Ford et al., 2010; Hall et al., 2007a; Nuccitelli et al., 2009; Vernier et al., 2003). The nsPEFs can treat tumors on external body surfaces with needle or plate electrodes and with the development of catheter electrodes internal organs can likely be treated with laparoscopic surgery. This therapy aims for well characterized cancer therapeutic targets including caspase-associated and caspase-independent apoptosis mechanisms as well as anti-angiogenesis, which influences invasion and metastasis. These studies provide answers to basic mechanistic questions of nsPEF-induced melanoma cell death; however, they present new questions regarding mechanism(s) for DNA damage, relative roles for caspase-associated apoptosis, caspase-independent apoptosis, and anti-angiogenic mechanisms for tumor death. Fewer questions can be raised about the potential for nsPEFs to provide a new, safe and non-toxic therapy for cancers.

Materials and methods

B16-F10 cells

Murine melanoma B16-F10 cells were obtained from ATCC (Manassas, VA, USA) and cultured as previously described (Nuccitelli et al., 2006).

Animals

In vivo experiments conformed to IACUC guidelines under applicable international laws and policies through Eastern Virginia Medical School. Hairless, female SKH-1 mice were injected subcutaneously with 100 μl PBS containing 1×10^6 B16-F10 cells. Two tumors induced simultaneously on the back of each mouse were randomly selected as either control or treated tumor. Treated tumors were exposed to nsPEFs using plate electrodes; control tumors were not. Tumors were removed at various times after treatment. Control and treated tumors were studied at each time (n = 6).

In vivo imaging

Before and after the treatment, melanomas were imaged daily by both transillumination and surface photography at 1.2× magnification. Tumor volumes were calculated using the formula for prolate spheroids (square of the width × length × 0.52): $V = 0.52 \times (D1 \times D2)^2$, where D1 and D2 are short and long tumor diameters, respectively in vivo using transillumination and surface photography. Volumes were confirmed by ultrasound.

nsPEF treatment

A pulser used a Blumlein line configuration and was designed and assembled at the Frank Reidy Research Center for Bioelectrics. It generated 300 ns pulses with a 30-ns rise time. One hundred pulses were applied to the treated tumor at 40 kV/cm and 0.5 Hz. The electrodes for electric field application, pulse generator, voltage and pulsing pattern of nsPEF were described previously (Nuccitelli et al., 2006).

Histology study

After nsPEF treatments both control and treated tumor were removed and fixed in 10% neutral buffered formalin prior to paraffin processing. Sections were stained with H&E and assessed microscopically for abnormal nuclear formation. One hundred nuclei were randomly selected and outlined in ten non-overlapping fields of each section. The area of nuclei was measured by the software MATLAB (The MathWorks, Natick, MA, USA) and summed as the mean ± SD for statistic analysis.

Tumor blood vessel analysis

Blood vessels (capillaries and venules) were counted in paraffin embedded tissue sections that were stained by H&E. The vessels were counted in an area of 0.74 mm^2 per field. Any red stained endothelial cells or endothelial clusters with the obvious lumen, clearly separate from immediately adjacent tumor cells and other connective tissue elements were considered a single vessel. Neither red blood cells nor vessel lumens were considered necessary for a structure to be defined as a vessel. Results were expressed as the highest number of vessels identified and counted within any single field.

DNA fragmentation

DNA was extracted by standard proteinase K and phenol/chloroform. Electrophoresis was performed in 1.8% agarose gel in TBE buffer (Tris-borate 89 mM, pH 8.3, EDTA 2 mM) at 30 V for 1 h. The DNA was visualized by ethidium bromide staining. B16-F10 cells incubated with etoposide (Calbiochem, San Diego, CA, USA) used as apoptosis positive control.

Immunofluorescent staining

Tumor sections were de-paraffinized and boiled in citrate buffer (pH 6.0) for 5 min for antigen retrieval. The tissue sections were placed in 3% hydrogen peroxide for 10 min to inactivate endogenous peroxidase. Tissues were blocked with goat serum, and incubated in a humidity tray with antibodies against phospho-histone H2AX (S139) (R&D Systems, Minneapolis, MN, USA; 1:500 dilution), caspase 3 (Cell Signaling Technology, Boston, MA, USA; 1:500 dilution), caspase 6 (Cell Signaling; 1:800), caspase 7 (BioVision, Mountain View, CA, USA; 1:400 dilution) for 2 h at room temperature. Caspase antibodies were used simultaneously. This was followed by incubation of a secondary antibody, Alexa Fluor-488-labeled goat anti-rabbit IgG (Invitrogen, Carlsbad, CA, USA; 1:250 dilution) for 30 min at room temperature in darkness. Cover slips were mounted with mounting media (Vector Laboratories, Burlingame, CA, USA), which contained DAPI (4′-6-diamidino-2-phenylindole) to identify the nuclei. Numbers of positive cells were determined by MATLAB software. Three sets of at least 100 cells under the microscope. Each experiment was performed twice.

TUNEL assay

Terminal deoxynucleotidyl transferase dUTP nick end labeling assay was done according to the protocol with ApopTag Red^{TM} *in Situ* (Chemicon, Temecula, CA, USA). Cells with TUNEL-positive nuclei with a cytoplasmic halo were counted as indicated above. For negative controls, no terminal transferase was added. Positive cells were determined by MATLAB software.

Immunoblot analysis

Proteins were resolved on 15% SDS-polyacrylamide gels and transferred to polyvinylidene difluoride (PVDF) membrane. Blots were pre-incubated in blocking buffer (5% non-fat dry milk, 1% Tween 20, in 20 mM TBS pH 8.0) for 1 h at room temperature, incubated with primary antibodies for VEGF (Santa Cruz, 1:200) or PD-ECGF (Santa Cruz Biotechnology, Inc, Santa Cruz, CA, USA; 1:200 dilution) in blocking buffer overnight at 4°C followed by incubation with anti-rabbit or anti-mouse secondary antibodies conjugated with horseradish peroxidase and detected by chemiluminescence and autoradiography using X-ray film.

Micro-vessel density measurement by CD31, CD34 and CD105 with immunohistochemistry (IHC)

The 5-μm-thick sections were deparaffinized in xylene, rehydrated and treated with 3% hydrogen peroxide for 20 min. Primary antibodies were used at following dilutions: monoclonal rat-anti-mouse CD31 (or PECAM-1, BD PharMingen), 1:50; rabbit polyclonal anti-CD34 (Biovision), 1:250; rat anti-CD105 (BD Pharmingen, San Diego, CA, USA; 1:200 dilution). Sections were covered with HRP-conjugated antibodies directed against rat or rabbit immunoglobulin. Non-specific staining was controlled by incubation with mouse or rabbit immunoglobulin instead of the specific primary antibody. 3-amino-9-ethyl-carbazole (AEC) was used as a chromogen, providing red depositions in situ.

Statistical analysis

Quantitative analysis was based on nuclear areas and positive immune-stained cells for phospho-H2AX, caspase and TUNEL between tumors with and without nsPEFs treatment. Samples were counted by MATLAB software using fluorescent staining. The number of positive cells was scored by counting three sets of at least 100 cells under a microscope. The differences between treated and control groups tested with two-tailed Student's t test and analysis of variance (ANOVA) (SPSS Statistical Program 15.0; SPSS Inc., Chicago, IL, USA).

Acknowledgements

We are grateful to Mr. Frank Reidy whose generosity and philanthropy supported this project. We also thank Wei Ren and Jie Liu who helped with in vivo tumor analysis and animal care. This work was in partial fulfillment of the PhD in Biomedical Sciences for Xinhua Chen at Old Dominion University.

References

Beebe, S.J., Fox, P.M., Rec, L.H., Buescher, E.S., Somers, K., and Schoenbach, K.H. (2002). Nanosecond pulsed electric field (nsPEF) effects on cells and tissues: apoptosis induction and tumor growth inhibition. IEEE Trans. Plasma Sci. *30*, 286–292.

Beebe, S.J., White, J., Blackmore, P.F., Deng, Y., Somers, K., and Schoenbach, K.H. (2003a). Diverse effects of nanosecond pulsed electric fields on cells and tissues. DNA Cell Biol. *22*, 785–796.

Beebe, S.J., Fox, P.M., Rec, L.J., Willis, E.L., and Schoenbach, K.H. (2003b). Nanosecond, high-intensity pulsed electric fields induce apoptosis in human cells. FASEB J. *17*, 1493–1495.

Beebe, S.J., Blackmore, P.F., White, J., Joshi, R.P., and Schoenbach, K.H. (2004). Nanosecond pulsed electric fields modulate cell function through intracellular signal transduction mechanisms. Physiol. Meas. *25*, 1077–1093.

Bergers, G., and Benjamin, L.E. (2003). Tumorigenesis and the angiogenic switch. Nat. Rev. Cancer *3*, 401–410.

Bland, K.L., Gass, J., and Klimberg, V.S. (2007). Radiofrequency, cryoablation, and other modalities for breast cancer ablation. Surg. Clin. North Am. *87*, 539–550.

Bonner, W.M., Redon, C.E., Dickey, J.S., Nakamura, A.J., Sedelnikova, O.A., Solier, S., and Pommier, Y. (2008). Gamma H2AX and cancer. Nat. Rev. Cancer. *8*, 957–967.

Chen, N., Garner, A.L., Chen, G., Jing, Y., Deng, Y., Swanson, R.J., Kolb, J.F., Beebe, S.J., Joshi, R.P., and Schoenbach, K.H. (2007). Nanosecond electric pulses penetrate the nucleus and enhance speckle formation. Biochem. Biophys. Res. Commun. *364*, 220–225.

Chen, X., Swanson, J.R., Kolb, J.F., Nuccitelli, R., and Schoenbach, K.H. (2009). Histopathology of normal skin and melanomas after nanosecond pulsed electric field treatment. Melanoma Res. doi: 10.1097/CMR.0b013e32832f1558.

Christmann, M., Tomicic, M.T., Roos, W.P., and Kaina, B. (2003). Mechanisms of human DNA repair: an update. Toxicology *193*, 3–34.

Daud, A.I., DeConti, R.C., Andrews, S. et al. (2008). Phase I trial of interleukin-12 plasmid electroporation in patients with metastatic melanoma. J. Clin. Oncol. *26*, 5896–5903.

Davalos, R.V., Mir, I.L., and Rubinsky, B. (2005). Tissue ablation with irreversible electroporation. Ann. Biomed. Eng. *33*, 223–231.

Deng, Y., and Chang, S. (2007). Roles of telemers and telemerase in genomic instability, senescence and cancer. Lab. Invest. *87*, 1071–1076.

Esser, A.T., Smith, K.C., Gowrishankar, T.R., and Weaver, J.C. (2009). Towards solid tumor treatment by nanosecond pulsed electric fields. Technol. Cancer Res. Treat. *8*, 289–306.

Fesik, S.W. (2005). Promoting apoptosis as a strategy for cancer drug discovery. Nat. Rev. Cancer 5: 876–885. Erratum in Nat. Rev. Cancer *5*, 995.

Fischer, U., Jänicke, R.U., and Schulze-Osthoff, K. (2003). Many cuts to ruin: a comprehensive update of caspase substrates. Cell Death Differ. *10*, 76–100.

Ford, W.E., Blackmore, P.F., Schoenbach, K.H., and Beebe, S.J. (2010). Nanosecond pulsed electric fields stimulate apoptosis with-

out release of pro-apoptotic factors from mitochondria in B16f10 melanoma. Arch. Biochem. Biophys. doi: 10.1016/j.abb.2010.03.008

Garon, E.B., Sawcer, D., Vernier, P.T., Tang, T., Sun, Y., Marcu, L., Gundersen, M.A., and Koeffler, H.P. (2007). In vitro and in vivo evaluation and a case report of intense nanosecond pulsed electric field as a local therapy for human malignancies. Int. J. Cancer *121*, 675–682.

Gehl, J. (2008). Electroporation for drug and gene delivery in the clinic: doctors go electric. Methods Mol. Biol. *423*, 351–359.

Gowrishankar, T.R., and Weaver, J.C. (2006). Electrical behavior and pore accumulation in a multicellular model for conventional and supra-electroporation. Biochem. Biophys. Res. Commun. *349*, 643–653.

Gowrishankar, T.R., Esser, A.T., Vasilkoski, Z., Smith, K.C., and Weaver, J.C. (2006). Microdosimetry for conventional and supra-electroporation in cells with organelles. Biochem. Biophys. Res. Commun. *341*, 1266–1276.

Green, D.R. (2005). Apoptotic pathways: ten minutes to dead. Cell *121*, 671–674.

Hair, P.S., Schoenbach, K.H., and Buescher, E.S. (2003). Sub-microsecond, intense pulsed electric field applications to cells show specificity of effects. Bioelectrochemistry *61*, 65–72.

Hall, E.H., Schoenbach, K.H., and Beebe, S.J. (2007a). Nanosecond pulsed electric fields induce apoptosis in p53-wildtype and p53-null HCT116 colon carcinoma cells. Apoptosis *12*, 1721–1731.

Hall, E.H., Schoenbach, K.H., and Beebe, S.J. (2007b). Nanosecond pulsed electric fields have differential effects on cells in the S-phase. DNA Cell Biol. *26*, 160–171.

Hanahan, D., and Weinberg, R.A. (2000). The hallmarks of cancer. Cell *100*, 57–70.

Heller, R., Jaroszeski, M.J., Glass, L.F., Messina, J.L., Rapaport, D.P., DeConti, R.C., Fenske, N.A., Gilbert, R.A., Mir, L.M., and Reintgen, D.S. (1996). Phase I/II trial for the treatment of cutaneous and subcutaneous tumors using electrochemotherapy. Cancer *77*, 964–971.

Hu, Q., Joshi, R.P., and Schoenbach, K.H. (2005). Simulations of nanopore formation and phosphatidylserine externalization in lipid membranes subjected to a high-intensity, ultrashort electric pulse. Phys. Rev. E. Stat. Nonlin. Soft Matter Phys. *72*, 031902.

Joshi, R.P., Nguyen, A., Sridhara, V., Hu, Q., Nuccitelli, R., Beebe, S.J., Kolb, J., and Schoenbach, K.H. (2007). Simulations of intracellular calcium release dynamics in response to a high-intensity, ultrashort electric pulse. Phys. Rev. E. Stat. Nonlin. Soft Matter Phys. *75*, 041920.

Kroemer, G., and Pouyssegur, J. (2008). Tumor cell metabolism: cancer's Achilles' heel. Cancer Cell *13*, 472–482.

Kroemer, G., Galluzzi, L., Vandenabeele, P. et al. (2009). Classification of cell death: recommendations of the Nomenclature Committee on Cell Death. Cell Death Differ. *16*, 3–11.

Lee, R.C., and Kolodney, M.S. (1987). Electrical injury mechanisms: electrical breakdown of cell membranes. Plast. Reconstr. Surg. *80*, 672–679.

Lee, R.C., Zhang, D., and Hannig, J. (2000). Biophysical injury mechanisms in electrical shock trauma. Annu. Rev. Biomed. Eng. *2*, 477–509.

Letai, A.G. (2008). Diagnosing and exploiting cancer's addiction to blocks in apoptosis. Nat. Rev. Cancer *8*, 121–132.

Maor, E., Ivorra, A., and Rubinsky, B. (2009). Non thermal irreversible electroporation: novel technology for vascular smooth muscle cells ablation. PLoS ONE *4*, e4757.

Mir, L.M., Orlowski, S., Belehradek, J. Jr, and Paoletti, C. (1991). Electrochemotherapy potentiation of antitumour effect of bleomycin by local electric pulses. Eur. J. Cancer *27*, 68–72.

Nuccitelli, R., Pliquett, U., Chen, X., Ford, W., James, S.R., Beebe, S.J., Kolb, J.F., and Schoenbach, K.H. (2006). Nanosecond pulsed electric fields cause melanomas to self-destruct. Biochem. Biophys. Res. Comm. *343*, 351–360.

Nuccitelli, R., Chen, X., Pakhomov, A.G. et al. (2009). A new pulsed electric field therapy for melanoma disrupts the tumor's blood supply and causes complete remission without recurrence. Int. J. Cancer *125*, 438–445.

Onik, G., Mikus, P., and Rubinsky, B. (2007). Irreversible electroporation: implications for prostate ablation. Technol. Cancer Res. Treat. *6*, 295–300.

Pakhomov, A.G., Bowman, A.M., Ibey, B.L., Andre, F.M., Pakhomova, O.N., and Schoenbach, K.H. (2009). Lipid nanopores can form a stable, ion channel-like conduction pathway in cell membrane. Biochem. Biophys. Res. Commun. *385*, 181–186.

Rogakou, E.P., Boon, C., Redon, C., and Bonner, W.M. (1999). Megabase chromatin domains involved in DNA double-strand breaks in vivo. J. Cell Biol. *146*, 905–916.

Schoenbach, K.H., Beebe, S.J., and Buescher, E.S. (2001). Intracellular effect of ultrashort electrical pulses. Bioelectromagnetics *22*, 440–448.

Sheikh, M.S., Burns, T.F., Huang, Y., Wu, G.S., Amundson, S., Brooks, K.S., Fornace, A.J. Jr, and el-Deiry, W.S. (1998). p53-dependent and -independent regulation of the death receptor KILLER/DR5 gene expression in response to genotoxic stress and tumor necrosis factor. Cancer Res. *58*, 1593–1598.

Shiloh, Y. (2003). ATM and related kinases: safeguarding genome integrity. Nat. Rev. Cancer *3*, 155–168.

Silva, M.T., do Vale, A., and dos Santos, N.M. (2008). Secondary necrosis in multicellular animals: an outcome of apoptosis with pathogenic implications. Apoptosis *13*, 463–482.

Stacey, M., Stickley, J., Fox, P., Statler, V., Schoenbach, K., Beebe, S.J., and Buescher, S. (2003). Differential effects in cells exposed to ultra-short, high intensity electric fields: cell survival, DNA damage, and cell cycle analysis. Mutat. Res. *542*, 65–75.

Stewart, D.A., Gowrishankar, T.R., and Weaver, J.C. (2004). Transport lattice approach to describing electroporation: use of local asymptotic model. IEEE Trans. Plasma Sci. *32*, 1696–1708.

Tekle, E., Oubrahim, H., Dzekunov, S.M., Kolb, J.F., Schoenbach, K.H., and Chock, P.B. (2005). Selective field effects on intracellular vacuoles and vesicle membranes with nanosecond electric pulses. Biophys. J. *89*, 274–284.

Torriglia, A., and Lepretre, C. (2009). LEI/L-DNase II: interplay between caspase-dependent and independent pathways. Front. Biosci. *14*, 4836–4847.

Vernier, P.T., Sun, Y., Marcu, L., Salemi, S., Craft, C.M., and Gundersen, M.A. (2003). Calcium bursts induced by nanosecond electric pulses. Biochem. Biophys. Res. Commun. *310*, 286–295.

Vernier, P.T., Ziegler, M.J., Sun, Y., Gundersen, M.A., and Tieleman, D.P. (2006). Nanopore-facilitated, voltage-driven phosphatidylserine translocation in lipid bilayers – in cells and *in silico*. Phys. Biol. *3*, 233–247.

Wang, S., Chen, J., Chen, M.T., Vernier, P.T., Gundersen, M.A., and Valderrábano, M. (2009). Cardiac myocyte excitation by ultrashort high-field pulses. Biophys. J. *96*, 1640–1648.

White, J.A., Blackmore, P.F., Schoenbach, K.H., and Beebe, S.J. (2004). Stimulation of capacitative calcium entry in HL-60 cells by nanosecond pulsed electric fields. J. Biol. Chem. *279*, 22964–22972.

Zhang, J., Blackmore, P.F., Hargrave, B.Y., Xiao, S., Beebe, S.J., and Schoenbach, K.H. (2008). Nanosecond pulse electric field (nanopulse): a novel non-ligand agonist for platelet activation. Arch. Biochem. Biophys. *471*, 240–248.